Electronic Supplementary Material (ESI) for Journal of Materials Chemistry

Supporting information

Effect of ZnS and CdS coating on the photovoltaic properties of $CuInS_2$-sensitized photoelectrodes

Guoping Xu, Shulin Ji, Chunhui Miao, Guodong Liu, and Changhui Ye

Key Laboratory of Materials Physics and Anhui Key Laboratory of Nanomaterials and Technology, Institute of Solid State Physics, Chinese Academy of Sciences, Hefei 230031, China.

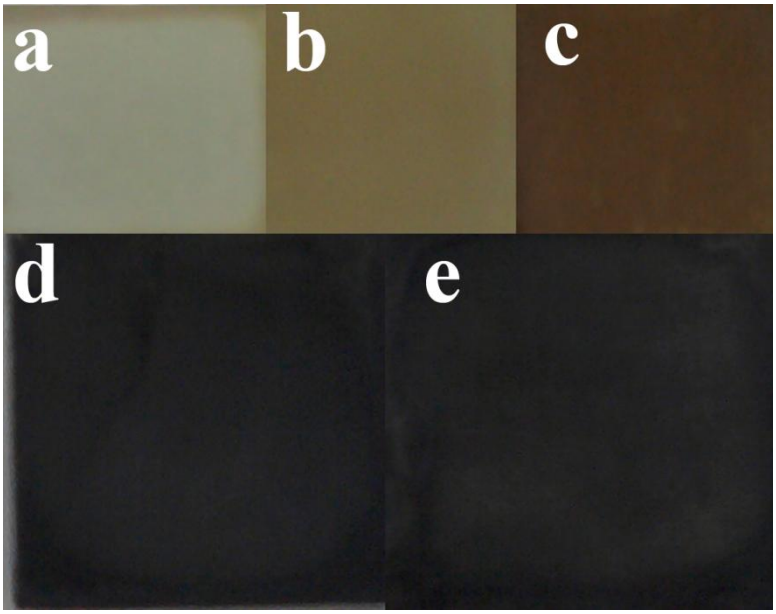

Fig. S1 Coating cycle repeated for 1(a), 2(b) and 3(c) times before sulfurization, respectively; typical samples after sulfurization with coating cycle repeated for 3 times, (d) 5 μm-sample and (e) 11 μm-sample

Fig. S1(a, b, c) show images of samples of coating cycle repeated 1-3 times before sulfurization. The heat treatment on a hot plate for 5 min evaporated the solvents and organic materials and led to reduction of copper (II). During the heat treatment, the surface color turned into a slight brown-hue and with the increase of the coating cycles, the color gradually deepened. It indicates the reduction of copper (II) to copper (I). Similarly, with the increase of the coating cycles, the color gradually changed from shallow dark into deep dark after sulfurization and annealing. Fig. 1(d,

e) show typical samples after sulfurization through a two-step heating temperature profile. After the heat treatment, the color turned into black which indicates CIS is an excellent light adsorption material.

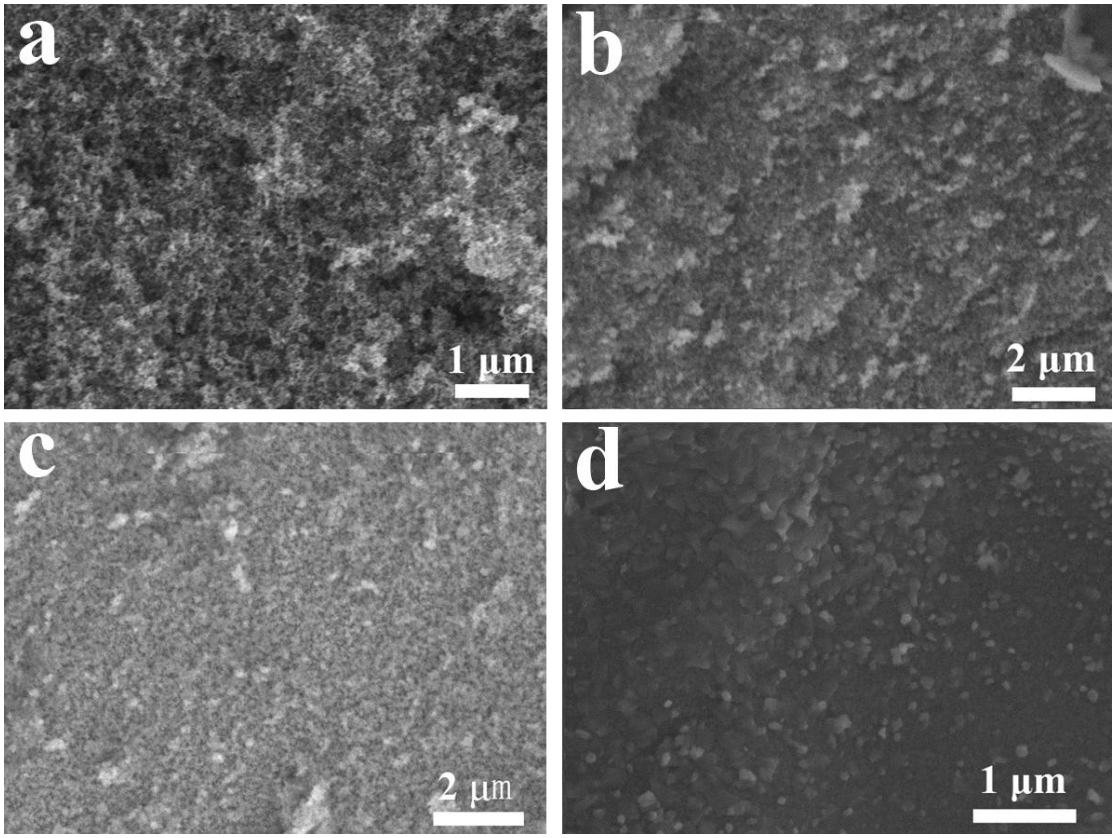

Fig. S2 TiO_2 particles (a), and CIS coated TiO_2 particles with 1 coating cycle (b), 2 coating cycles (c), and 4 coating cycles (d) after sulfurization, respectively

Fig. S2 depicts TiO_2 films before and after CIS coating with different coating cycles after sulfurization. The grain size of the CIS gradually grew bigger and a high coverage on TiO_2 surface was displayed.

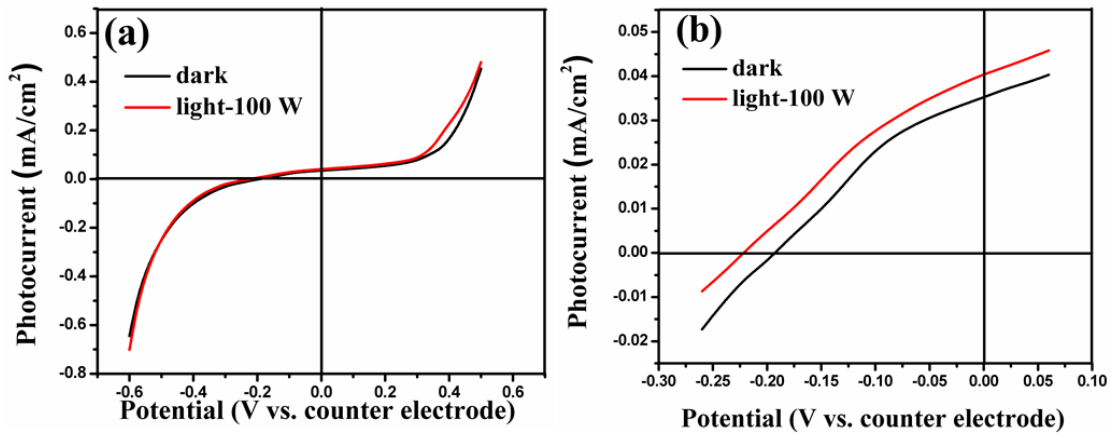

Fig. S3 I-V curves of TiO_2/ZnS/CIS electrodes with thickness of 11μm (a) and the enlargement of photovoltaic I-V plots in the second quadrant of Fig. S3(a)

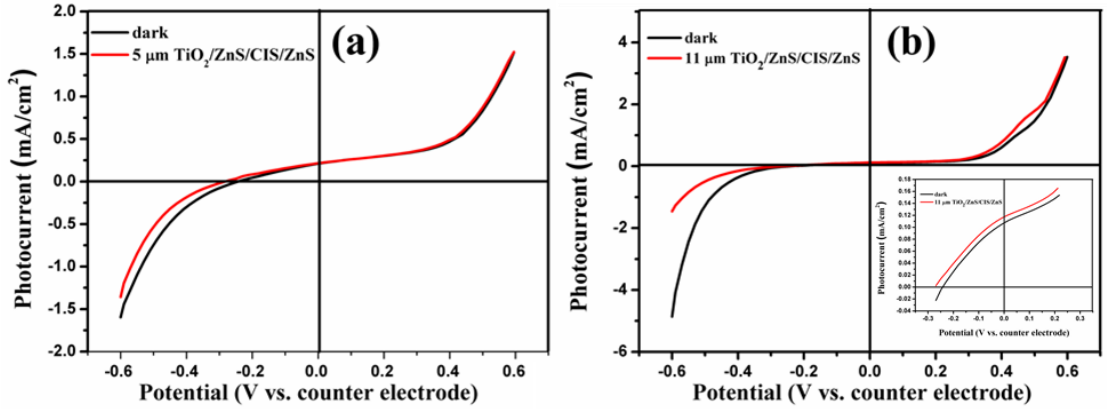

Fig. S4 I-V curves of TiO_2/ZnS/CIS/ZnS electrodes with thickness of 5 μm (a) and 11 μm (b), the inset is the enlargment of photovoltaic I-V plots in the second quadrant in Fig. S4(b).

Fig. S5 shows the I-V curves of a 11 μm-sample under illumination of 100 W/m^2 with 504 and 604 nm LED, respectively. It indicates that the CIS layer plays a leading role for the photoelectrochemical response.

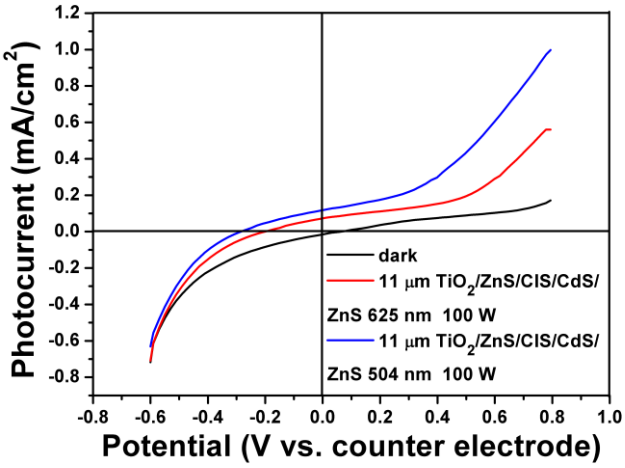

Fig. S5 5 μm-sample with TiO_2/ZnS/CIS/CdS/ZnS configuration irradiated under the 504 nm and 625 nm LED at the same light power intensity, respectively.

Table SI

	Early reported conduction band edge vs vacuum level (eV)	Early reported conduction band edge vs SHE (eV)	Our tested conduction band edge (eV) obtained from the CV vs SHE	Our tested conduction band edge (eV) obtained from the CV vs vacuum level
TiO_2	-4.2	-0.3	-0.74	-3.76
CIS	-4.1	-0.4	-0.85	-3.65
CdS	-3.8	-0.7	-1.15	-3.35

SHE is 4.5 eV below the vacuum level

Oxdiation reaction of S^{2-}/ SO_3^{2-} in the solution:

$S^{2-}+2h^{+}\rightarrow S$ -0.476 V vs SHE, 25°C (1)

$SO_3^{2-}+2OH^{-}+2h^{+}\rightarrow SO_4^{2-}+H_2O$ -0.93 V vs SHE, 25°C (2)

S^{2-} vs vacuum level:

-0.476+4.5=4.024 eV below vacuum level

SO_3^{2-} vs vacuum level:

-0.93+4.5=3.57 eV below vacuum level

RHE: $E_{RHE}=E_0$-0.0592*pH=0-0.6808=-0.6808 eV

Electrochemical studies

Electrochemical measurements were performed at room temperature on IM6ex (Zahner, Germany) electrochemical workstation.

Cyclic voltammetry (CV) and electrochemical impedance spectrum (EIS) were performed with a Zahner IM6eX system. Cells were measured in two or three-electrode configuration in the dark with 10 mV AC perturbation over a frequency range of 0.1 Hz to 100 kHz.

TiO_2 compact layer: A compact TiO_2 layer was deposited onto FTO by the $TiCl_4$ treatment in order to avoid the short circuit between FTO and electrolyte. CV and EIS, performed in 0.1 M NaOH in three-electrode configuration with a saturated calomel electrode (SCE) as reference electrode and a Pt sheet as counter electrode were employed to analyze the influence of the compact TiO_2 layer. Fig. S6(a) shows the cyclic voltammograms of 11 μm TiO_2 electrodes with and without a compact layer. For both, at more negative potentials than -0.6 V, faradaic currents rises in the cathodic direction due to charge accumulation while at less than -0.6 V faradaic currents tends to stabilization in agreement with CV curves presented elsewhere. Clearly, faradaic current falls sharply in the accumulation region with a compact layer which plays a role of blocking the direct contact between FTO and the electrolyte. Fig. 6(b) illustrates the charge transfer resistance (R_{ct}) obtained from a semi-arc in the low frequency region by fitting the EIS data. The values of R_{ct} decrease at more negative potentials than -0.2 V in the cathodic direction due to charge accumulation which agrees with cathodic current increased shown in CVs in Fig. 6(a). At certain potentials in the range of -0.2 to 0.5 V, the values appear to be stable with or without a compact layer which implies the current is undisturbed. It is consistent with the performance of faradaic currents in the anodic direction in Fig. 6(a). At potential more than 0.5 V, the values decrease again because of an increase of current density in the anodic direction. Based on the above, the compact layer can effectively block the FTO electrode.

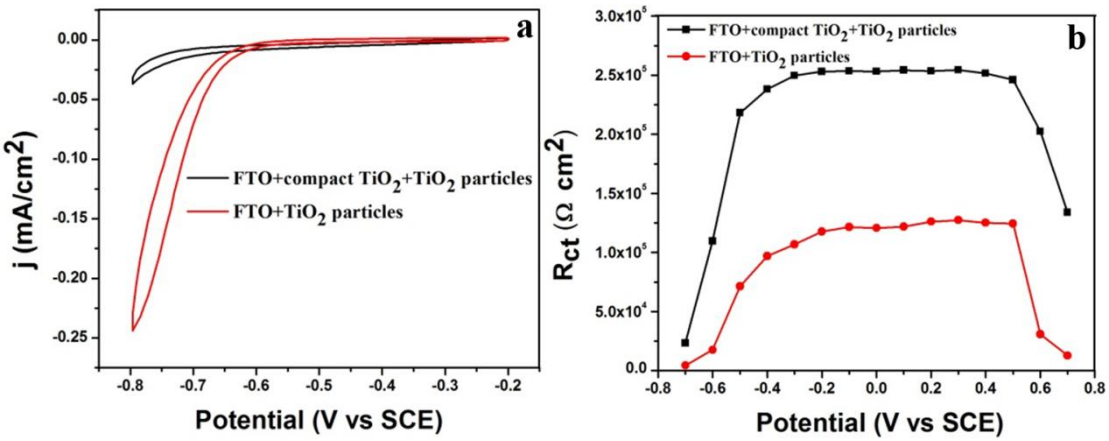

Fig. S6 Cyclic voltammetry at a scanning rate of 20 mV/s (a) and charge transfer resistance (R_{ct}) for TiO_2 electrode with and without a TiO_2 compact layer (b).

ZnS Pre-treatment:

The effective passivation with ZnS pre-treatment has been demonstrated by EIS. The TiO_2 electrodes were passivated by ZnS pre-treatment through the SILAR method. EIS was performed in 1 M Na_2S +0.1 M S + 1 M NaOH aqueous solution (polysulfide). Two different constructions, FTO/compact layer/TiO_2particles (C+P), FTO/compact layer/TiO_2 particles/ZnS (C+P+ZnS) were prepared as work electrodes. Fig. S7 shows impedance spectra and R_{ct} obtained from a semi-arc in the low frequency region by fitting the EIS data. Fig. S7(a) illustrates the typical Nyquist plots of the electrodes obtained in the accumulation region with and without ZnS pre-treatment. In all cases, R_{ct} can reach the maximum close to the open circuit potential (OCP) while follow an exponentially decreasing behavior away from the OCP. However, an increase in the R_{ct} is observed at each corresponding potential after the electrodes modified by ZnS. It indicates that the ZnS pre-treatment can block the TiO_2 surface and prevent recombination with the electrolyte and lead to a rise in R_{ct} in agreement with the previous research. Therefore, the pre-treatment process can make contribution to the photocurrent due to a better blockage of the TiO_2 surface prior to the sensitization of the electrodes with CIS. Although the TiO_2 was passivated by the ZnS pre-treatment, the ZnS post treatment plays an important role for the improvement of the photovoltaic performance.

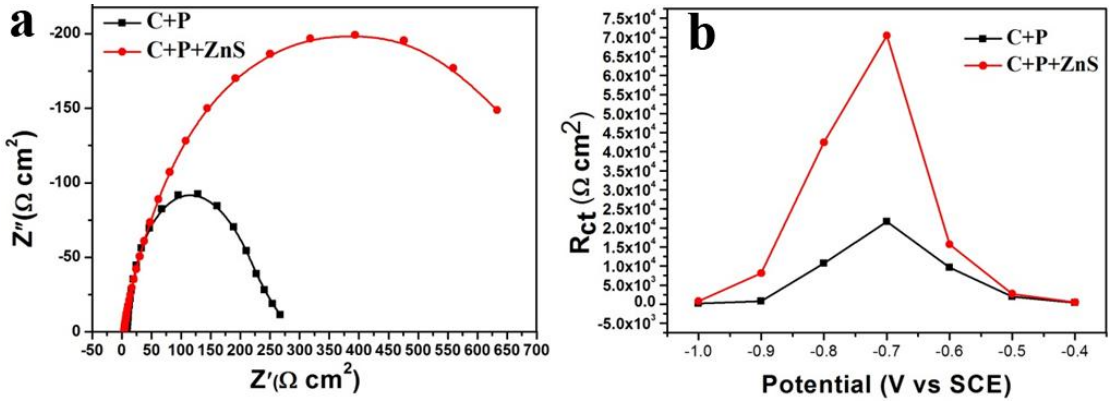

Fig. S7 Electrochemical impedance spectra data in dark were obtained in the range from 0.1 Hz to 100 000 Hz at an applied potential of -1 V vs SCE (a) and a series of values of R_{ct} at applied potential from -1 V to -0.4 V were calculated by fitting the EIS data.

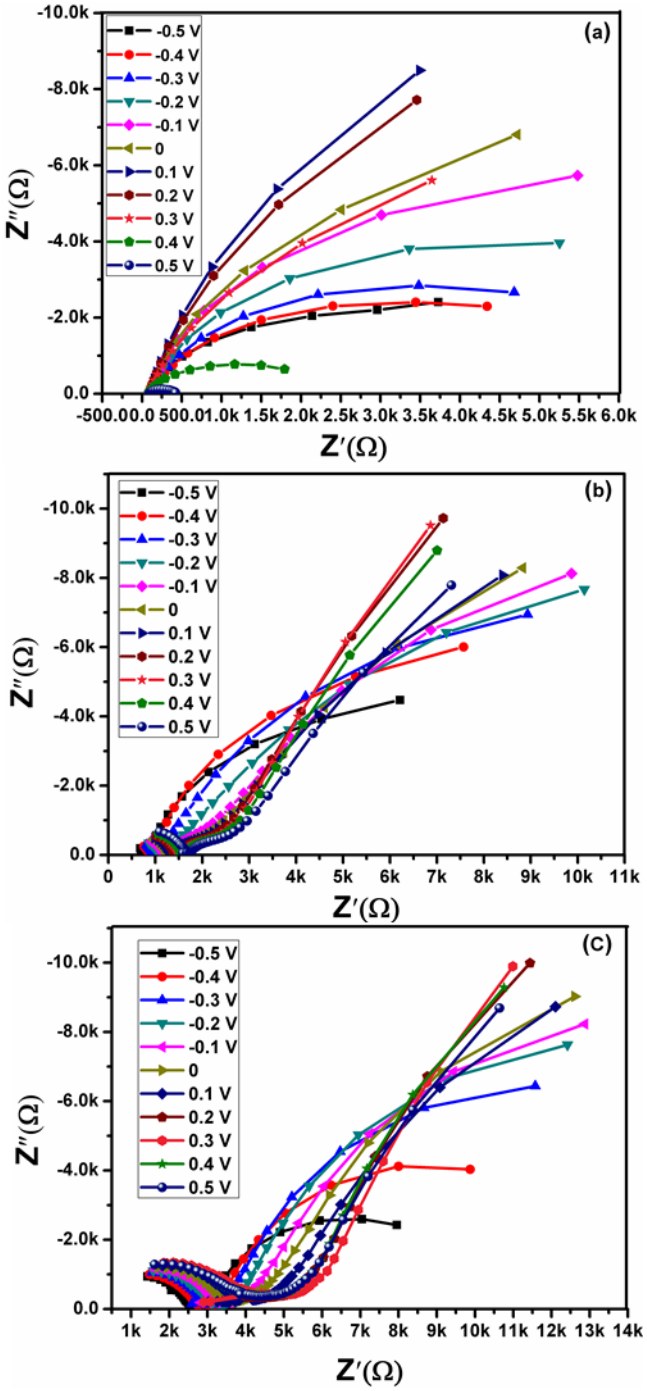

Fig. S8 Nyquist plots of theTiO_2/ZnS/CIS (a), TiO_2/ZnS/CIS/CdS (b), and TiO_2/ZnS/CIS /CdS/ZnS electrodes (c)